Chapter 5

In silico based Molecular Docking, Drug-likeliness and DFT study for the evaluation of target-drug interaction, ADME, druggability, and chemical reactivity of 4-FPAC

The *in silico* drug designing is a computer-aided high throughput method of drug discovery and development. The term *"in silico"* stands for *"within a computer"* shows analogy with *in vivo*, *in vitro,* and *in situ.* The *in silico* based drug designing and development process has overcome the tedious, time consuming, and expensive process of traditional drug discovery and became an essential part of every aspect of drug discovery from the selection of target to generation and evaluation of lead compound (Le et al., 2015). In *in silico* based drug designing, ligands with the desired property are designed based on literature-based pharmacological data by using bioinformatics tools or searched from the virtual library (virtual screening), which is specific towards target molecule. However, here in this study, ligands were chemically synthesized based on literature. These ligands with desired properties were used for initial Hit identification by High throughput screening method (HTS), which includes calculations of *in vitro* based IC_{50} concentrations. Potential hits with promiscuous properties are further filtered based on their pharmacokinetic and pharmacodynamic properties. These properties explain the "drug-likeliness" of the hits, which is based on the ADME and Rule of Five develop by Lipinski (Lipinski et al., 1997). ADME stands for Absorption, Distribution, Metabolism, and Excretion, and applied to check the oral bioavailability of compound, hepatotoxicity, and human intestinal absorption of compounds. Similarly, Rule of Five (clogP≤5, molecular weight≤500, the number of hydrogen bond acceptors≤10 and donor≤5), is also used to check the drug-likeliness of the compound in terms of lipophilicity, critical molecular weight and chemical structure, required for crossing the blood-brain barrier (BBB). The compound violating more than one of these rules will be poor in terms of bioavailability and therefore, for "lead optimization," the compounds which satisfy these criteria will only be taken for molecular docking (Sakkiah and Lee, 2012).

Molecular docking is an automated computer algorithm that determines how a compound will bind at the active site of the target macromolecule. Docking algorithm puts the ligand in many different orientations in the active site of the target macromolecule and predicts the pose with

the lowest energy and then computes a "score" for each pose. The score is based on their van der Walls interactions, electrostatic interactions, solvation effects, and entropic effects between ligand and target (Gohlke and Klebe, 2002). Since target and protein both are flexible, it works as a "hand and gloves" phenomenon where both adjust themselves to achieve the "best fit" orientation as well as confirmation. Molecular Docking, therefore, aims to achieve an optimized confirmation and orientation so that the free energy of the system gets minimized (Jorgensen, 1991).

In standard Virtual Docking, the ligands are docked into the binding site of the receptor where the receptor held rigidly, and the ligand is free to move, but this is not as true since many of the protein undergo side chain or back-bone movement during binding of ligands. These changes allow the receptor to undergo alterations in their binding site shape and binding mode so that it can accommodate ligand more precisely. This mode of docking is known as "induced fit" in which the van der Walls radii is reduced, and the coulomb-vdW cut-off was increased with temporary deletion of the highly flexible side chain of the receptor (Schrodinger, 2015).

However, DFT (Density Functional Theory) calculations is used for the prediction of the electronic molecular features of the compound, which defines the chemical, physical, and biological reactivity of the compound. The DFT calculations include the molecular electrostatic potential (MESP) map generation, which is a three-dimensional mapping of a compound that visualizes the charge distribution of the compound and helps in the prediction of reactive polarity and behavior of compound. The other remarkable guideline to predict the electronic property and reactivity of any compound based on the DFT calculation is the frontier molecular orbital density (FMOs) field, i.e., HOMO-LUMO, where, HOMO stands for the highest occupied molecular orbital and correlated with the electron-donating ability of the molecule. In contrast, LUMO stands for the lowest unoccupied molecular orbital and correlated with the electron-accepting ability. The frontier molecular orbital energies are used to narrate the electron density cloud around the molecule. High LUMO energy is the favorite site for the nucleophilic attack, and high HOMO energy is predictive of high electrophilic attack. A large HOMO-LUMO gap is related to high kinetic stability and low chemical reactivity and vice versa (Lee et al., 1988). Based on the HOMO and LUMO energies and their energy gap, chemical as well physical nature of the compound can also be analyzed, including hardness, softness, ionization potential, electron affinity, electronegativity and chemical potential of the compound. Thus, in modern drug designing and development, molecular docking and DFT study of *in silico* are routinely used to

evaluate drug-target interactions, the position of the reactive site, and biological reactivity of the novel compounds.

Based on the *in vitro* studies of previous chapters, it was observed that 4-fluorophenylacetamide-acetyl coumarin (4-FPAC) exerts anti-proliferative, anti-metastasis, and anti-angiogenic effects in the A549 human lung cancer cell line. 4-FPAC executes it's effect by activating the intrinsic as well extrinsic pathway of apoptosis, arresting cell cycle at G0/G1 phase, reducing the Epithelial to Mesenchymal transition by downregulating the Snail, hampering the invasion by the minimizing the MMPs, and prevent vascularization by downregulating the IL-8 in the A549 cell line. At the molecular level, DNA damage-induced p53 was found to be the major downstream regulator and PI3K/AKT/NF-κB signaling pathway as a major targeted pathway for the anticancer activity of 4-FPAC.

Therefore, based on the literature as well as on the results of *in vitro* study, the compound 4-FPAC was evaluated using *in silico* based molecular docking study to unravel its effect on the key target proteins (*viz.*, p53, BAX, caspase 8, caspase 3, SNAIL, VEGFR, PTEN, and HIF-1α) that regulate the proliferation, metastasis, and angiogenesis in A549 cell line. DFT calculations were used to characterize the electronic and structural features of the 4-fluorophenylacetamide-acetyl coumarin, as it is a initial step for future studies of the molecular docking of the compound to elucidate the reaction mechanism of the compound, targeting a future increase in its action pharmacological. Similarly, The pharmacological potential of the compound was evaluated using Drug-likeliness and ADME property using some knowledge-based set of rules to investigate its safety level if consumed.

COMPUTATIONAL METHODS

Electronic Properties

Density Functional Theory Analysis (HOMO-LUMO and MESP map)

The molecular property and reactivity of 4-FPAC were evaluated using density functional theory (DFT) based analysis of molecular electrostatic properties. DFT calculations are used for studying the electronic molecular features to define a molecular electrostatic map, with the electron density and frontier molecular orbital (FMOs) density fields (HOMO, LUMO), that can predict the molecular properties and biological activity of the compound. MESP maps (MESP isoenergy contours generated at -30.0kcal/mol) and HOMO and LUMO were computed using Jaguar (Schrödinger), an *ab initio* quantum chemical program, version 9.8 Schrödinger, installed

on Intel core i7-2600 CPU @ 3.40GHZ by applying Becke's three-parameter exchange potential and the Lee-Yang-Parr correlation functional (B3LYP), using a basis set 631G**++ level (Gill et al., 1992). For stimulating physiological conditions, energy calculations were performed in an aqueous environment using "Poisson Boltzmann Finite" (PBF) solvation. For a better understanding of the structure, activity, and dynamics of a molecule, electronic calculations play a significant role and also present a computational approach to drug designing.

ADME and Drug- Likeliness Prediction

4-FPAC was evaluated for its drug-likeliness through ADME properties using the QikProp module (ADME; Adsorption, Distribution, Metabolism, Excretion predictions, version 4.4, Schrodinger, LLC, New York, 2015) inbuilt in the Schrödinger software suite. This software helps in predicting pharmacokinetics and pharmacodynamics of derivative and shows it's pharmaceutical relevance as a drug candidate molecule. The candidate molecules are assessed based on the biological properties such as the predicted octanol/water partition coefficient (QPlogPo/w), octanol/gas partition coefficient (QPlogPoct), water/gas partition coefficient (QPlogPw), brain/blood partition coefficient (QPlogBB), aqueous solubility (QPlogS), apparent Caco-2 cell permeability in nm/sec (QPPCaco) and apparent MDCK cell permeability in nm/sec (QPPMDCK). The overall CNS activity, the human serum albumin binding (QPlogKhsa), the skin permeability (QPlogKp), and the cardiac activity (QPlogHERG) were also predicted using *in silico* based ADME study (Table 5.3). Evaluation of drug-likeness of a compound was based on the number of violations of Lipinski's Rule of Five, which is critical for rational drug design, which includes the molecular weight of the compound, number of H-bond donors, number of H-bond acceptors and lipophilicity (Lipinski et al., 1997).

MOLECULAR DOCKING

All computational studies were carried out using Workstations from Supermicro with configurations of Intel® core™ I7p-2600 CPU @ 3.40 GHz, Operating System CentOS 6.3, Desktop from Lenovo with configurations of Intel ® Core ™ 2 Duo CPU E7300@2.66GHZ.

Ligand preparation

The structure of the compound 4-FPAC was generated using ChemDraw ultra 2012. The sketched ligand structure was prepared using LigPrep, an application of Maestro (LigPrep, version 3.4, Schrödinger, LLC, New York, NY, 2015). The database ligands were prepared, and different ionization states were generated at pH 7.0±2.0 using an epik state; a enumerates ligand

protonation states and tautomers in biological conditions, version 3.2 (Schrödinger, LLC, New York, NY, 2015) and the substantial penalties for high energy ionization of tautomer states were removed. Geometry, and charges (partial atomic charges) were optimized using the optimized potentials for liquid simulations-2005 (OPLS-2005) force field. In the default constraint parameters, as a scaling van der Walls radius of 1.0 Å for the protein with a partial atomic charge set at less than 0.25 Å. LigPrep is a utility in the Schrödinger software suite that ensures optimization of ligand geometry, minimizes the energy of 3D structure, and gives the best tautomeric and steric isomer with minimized energy for the docking.

Protein preparation

X-ray crystallographic structure of target proteins, i.e., p53, BAX, caspase 8, caspase 3, VEGFR, SNAIL, PTEN and HIF-1α were retrieved from Protein Data Bank (PDB). The respective PDB IDs 5LGY, 2K7W, 4ZBW, 4QTX, 5EW3, 4QLI, 5BZX, and 5L9B were prepared for docking using protein preparation wizard (Schrödinger Suite 2015 Protein Preparation Wizard Schrödinger, LLC, New York, 2014) in Maestro, (Schrödinger, LLC, New York, NY, 2015). Protein preparation is a multistep process in which wizard adds missing bond as well as side chains, assigns correct bond order and charges, removes any crystallographic water whereas, hydrogens remain unstrained, and geometry of the input protein remains unaltered; instead it checks for any problems in the protein structure and corrects them. In order to determine and optimize the atomic charges, the OPLS-force field of the Schrödinger software was used, which contains different parameters for treating different atoms. Additionally, the energy was minimized until the average root mean square deviation of non-hydrogen atoms reached 0.30 Å, it will help any structural deviations.

Active site prediction

The active site residues of PDB IDs: p53 (Vainer et al., 2016), BAX (Gavathiotis et al., 2008), caspase 8 (Shen et al., 2015), caspase 3 (Prashanth et al., 2019), VEGFR (Markovic-Mueller et al., 2017), SNAIL (Prokop et al., 2013) PTEN (Lee et al., 2015) and HIF-1α (Chowdhury et al., 2016), were obtained from the literature. Once the structure was optimized, the receptor grid was generated, which encloses the active site of amino acids. For generating the receptor-grid, the scaling van der Walls radii was set at 1.0 Å and enclosed in the bounding box set at 20 Å.

Induced Fit Docking

To further confirm the docking results, "Induced Fit Docking" (mixed molecular docking/molecular dynamics protocol) was run using the whole set of docking protocol. It allows receptors to kept flexible, along with ligand (Singh et al. 2012). The same default parameters, as mentioned in the standard Glide XP docking method, were used. Ligand and protein were docked with Schrödinger's induced fit protocol by using Glide software to exhaustively consider possible binding modes and the associated conformational changes within the receptor's active sites. This unique procedure allows the prediction of active site geometries with minimal expense yet quickly. The graphical user interface for the Schrödinger software, Maestro, was used for the execution of induced fit simulations and interpretation of the result (Schrödinger internet). Once the receptor grid was generated, the ligand 4-FPAC was docked to the receptor using Glide (version 6.7) docking protocol with default parameters under the Extra precision (XP) model (Jayaraman and Jamil, 2014).

RESULT

DENSITY FUNCTIONAL THEORY CALCULATIONS

Frontier Molecular Orbitals (FMOs) density field of 4-FPAC

HOMO and LUMO orbitals play a significant role in predicting the chemical nature, reactivity, bioactivity, and stability of the compound. The DFT calculations were done using Jaguar version 9.8 of the Schrödinger software suite and observed that in 4-FPAC, the HOMO orbitals are located on the 4-Fluorobenzene ring, and LUMO orbitals are located on the 3-acetyl coumarin ring, both distributed around the Amine, Oxygen, Carbon, and Fluorine groups, indicating the participation of these moieties during protein-ligand interactions (Figure 5.1). The calculated HOMO, LUMO, and HOMO-LUMO energy gap for 4-FPAC are -0.2430eV, -0.1052eV, and -0.1378eV, respectively (Table 5.1). These energies also characterize the electrophilic or nucleophilic nature of a compound (Eroglu and Türkmen, 2007). Since the E_{LUMO} and E_{HOMO} are responsible for charge transfer in a chemical reaction, the compound with lower gap energy is generally more polarizable as well as associated with high chemical reactivity and low kinetic stability. The molecules which are associated with such properties are termed as a soft molecule (Powell et al., 2004).

Based on the Koopman's theorem for closed-shell molecules, the global reactivity descriptors were also analyzed by using HOMO and LUMO energies of the compound (Pearson, 1986).

These quantum chemical descriptors are Ionization Potential (I), Electron Affinity (A), Softness (S), Chemical Hardness (H), Chemical Potential (μ), Electronegativity (X) and Electrophilic Index (ω). As presented in Table 5.1.1, the Ionization potential, electron affinity, softness, chemical hardness, chemical potential, electronegativity, and electrophilic index for 4-FPAC were found to be 0.2430eV, 0.1052eV, 7.26eV, 0.0689eV, -0.174eV, 0.174eV and 0.219eV respectively.

Molecular Electrostatic Potential (MESP) of 4-FPAC

In general, the different values of the electrostatic potential are represented by different colors. It is widely accepted that the negative (red) and the positive (blue) potential regions in a mapped MESP represent regions susceptible to approach by electrophiles and nucleophiles, respectively. The color code of these maps ranges between -192.2281 a.u (deepest red) and -23.1788 a.u. (deepest blue). Most positive electro potential region colored deepest blue (most nucleophilic site) and the most negative electro potential region colored deepest red (most electrophilic site) (Govindrajan et al., 2012). In the MESP map of 4-FPAC (Figure 5.2), the region having the most negative potentials are over the Oxygen and Fluorine atom, and the most positive region is present over the Hydrogen atom and the Methyl group.

Drug-Likeliness and ADME Prediction of 4-FPAC

The ADME property of any novel derivative is calculated to get an initiative that the derivative has the competency to enter into an advanced stage of the drug development process and become a future candidate for treatment. With this aim, the Drug-likeliness properties such as molecular weight <500, clogP not greater than 5 with <5 hydrogen bond donors, and >10 hydrogen bond acceptors were assessed using the criteria set by Lipinski's Rule of Five (Lipinski et al., 1997). The result revealed that, 4-FPAC has a molecular weight of 355.3, hydrogen bond donor 1, hydrogen bond acceptor 7.5 and QPlogPo/w octanol-water partition coefficient, 2.329 (Table 5.3). All the properties are under the acceptable range and satisfy the criteria set for drug-likeliness with Lipinski's Rule of Five.

The octanol/water partition coefficient and water solubility are the crucial parameters for the estimation of absorption and distribution of drugs within the body. The brain-blood partition coefficient is also an important criterion of absorption and distribution for predicting the ability of the compound to penetrate the blood-brain barrier. The result obtained revealed that QPlogPo/w, QPlogS and QPlogBB of 4-FPAC, are in the accepted range, i.e., 2.329, -4.519, and -1.271(Table 5.3). Similarly, the Caco-2 cell permeability in nm/sec, which is an essential factor

in regulating the drug metabolism and its transport across membranes, is found to be 319.6. The Caco-2 cells are the model for the gut-blood barrier and can give an early indication of the likelihood of compound being absorbed in the gastrointestinal tract (GI). The MDCK cells are considered a good mimic of the blood-brain barrier and a drug that has permeability less than 500nm/sec considered to have good druggability. The MDCK cell permeability of 4-FPAC is found to be 260.94 nm/sec. The predicted IC_{50} value for the blockage of the HERG K^+channel was -6.35 (above -5 hence, slightly lower than the accepted range). HERG or potassium channel gives an early indication of potential adverse cardiac toxicity. The percentage of human oral absorption was computed as 85.41%. The other parameters, such as QPlogKp (the skin permeability), #rtvFG (number of the reactive functional group), SASA (Total solvent accessible surface area), FOSA (a hydrophobic component of the SASA), FISA (a hydrophilic component of the SASA), and PSA (a component of the SASA, Polar nitrogen and oxygen van der Waals surface area) were also predicted and found to be under the acceptable range except for the QPlogKhsa (human serum albumin binding efficiency), which, however, was found marginally lower (Table 5.3).

The compound that satisfies all the criteria of ADME, and Lipinski's Rule of Five, considered as a drug-like molecule (Table 5.3). The maximum four criteria of Lipinski's Rule should satisfy to be a good candidate drug with an acceptable range of ADME descriptors. The drug in question, 4-FPAC could satisfy all the criteria of Lipinski's Rule and ADME descriptors, hence, it is under the acceptable range for human usage.

MOLECULAR DOCKING

4-FPAC was docked against all the PDB IDs; 5LGY (p53), 2K7W (BAX), 4ZBW (caspase 8), 4QTX (caspase 3), 5EW3 (VEGFR), 4QLI (SNAIL), 5BZX (PTEN) and 5L9B (HIF-1α), and their affinities were evaluated. The details of this analysis are presented below.

p53

The P53 is the 'guardian gene' of the cell that activates the DNA repair as well as the death process in response to DNA damage (Strachan and Read, 1999). *In vitro* based studies (Chapters 2 and 3) have revealed that p53 is the major regulator of 4-FPAC induced cell death as well as metastasis process in the A549 cell line. Through *in silico* based molecular docking study, it was observed that 4-FPAC docked efficiently with p53 (5LGY) at the active site and generated a docking score of -5.89kcal/mol, Glide energy of -48kcal/mol, Glide emodel of -67.9kJ/mol and

IFD score of -420kcal/mol. Ligand interacts with the targeted protein, p53 by six hydrogens (H-bond) and two pi-cation interactions, *viz.*, Lys132 -H bond with the oxygen atom of ligand at a distance of 2.60 Å, Arg273 -H bond with the oxygen atom of ligand at a distance of 2.13 Å, Arg248 - H bond with the NH atom of the ligand at a distance of 1.91 Å, Arg280 and Ala276 - NH interact with the 3-Oxo-butyraldehyde group of the ligand at a distance of 2.38 Å, 2.07 Å and 1.85 Å. A 2H-Chromene moiety of ligand forms pi-cation with Arg273 at a distance of 4.6 Å and 5.8 Å (Figure 5.3, Table 5.2). The negative value of the docking score and interactions with the 4-FPAC might be responsible for the binding site competition with Mdm2 and activation of the p53 to perform its function.

BAX

BAX is a pro-apoptotic member of a BCL-2 gene family whose ratio to BCL-2 determines the fate of the cell, to die, or to survive. The increased expression ratio of BAX to BCL-2 or pro-apoptotic to anti-apoptotic pushes the cell toward apoptotic death (Raisova et al., 2001). To permeabilize the mitochondrial membrane, BAX binds to the outer membrane of the mitochondria as a monomeric unit, and within seconds it oligomerizes and forms pore, which helps in the release of cytochrome c to mediate apoptosis. However, when BCL-2 is present in higher concentrations than BAX, it dissociates the BAX oligomers from the mitochondrial outer membrane and pushes cells toward survival (Subburaj et al., 2015). Therefore, a strong binding or interaction of derivative (4-FPAC) with the protein (PDB ID; 2K7W) can increase or decrease the oligomerization process and thereby activation of the BAX to act on cells. 4-FPAC interact with 2K7W at the active site amino acid residue and generated a docking score of -11.7kcal/mol, Glide energy of -50.78kcal/mol, Glide emodel of -65.94kJ/mol and IFD score of -436.558kcal/mol (Figure 5.3, Table 5.2).

The protein interacts with the 4-FPAC through two hydrogen bond (H-bond) and three pi-pi stacking; Trp17 -H-bond between NH group of the ligand with the oxygen atom of the amino acid at a distance of 2.04 Å, Gly166 -H bond between oxygen group of ligand interact with the methylamine moiety of the amino acid at the distance of 1.87 Å, Phe165 -2-Methylene-2H-chromene and F-benzene moieties at a distance of 4.07, 3.87 and 4.78 Å (Figure 5.3, Table 5.2.1). In the earlier chapter (Chapter 2), *in vitro* analysis revealed that the increased expression of *BAX* was responsible for the induction of apoptosis in the A549 cell line. Therefore, the interaction of BAX with 4-FPAC induces significant conformation changes, which leads to the oligomerization and activation of BAX to perform its apoptotic function.

Caspase 8

The initiator caspase of the extrinsic pathway of apoptosis, caspase 8, activates its downstream mediator and an effector caspase, i.e., caspase 3, whose activation initiates the process of apoptosis. *In vitro* study highlighted in the earlier chapter (Chapter 2), confirmed that the derivative 4-FPAC activates the extrinsic pathway of apoptosis by altering the expression of TNF-α and its downstream mediators. Nonetheless, the effect of the 4-FPAC was either due to the direct contact or due to upstream mediator, was not confirmed, therefore, here in this chapter, the *in silico* based molecular docking study was performed to investigate its detailed mechanism of action. Caspase 8 (4ZBW) interacted with 4-FPAC with two hydrogen bonds (Figure 5.3, Table 5.2.1) between Asn138 -the 3-Oxo-butyraldehyde group of the ligand interacts with the NH group of the amino acid at a distance of 2.48 Å and Ser109 -NH group of the ligand and oxygen atom of the group of 3-Acetyl-5,6-dihydro-pyran-2-one moiety at a distance of 2.53 Å. This interaction leads to the generation of a docking score of -5.563kcal/mol, Glide energy of -42.05kcal/mol, Glide emodel of -54.187kJ/mol and IFD score of -441.53kcal/mol (Figure 5.3, Table 5.2). This study confirmed the direct activation of caspase 8 with the 4-FPAC to activate its downstream mediator caspase 3 to initiate the process of apoptosis.

Caspase 3

Caspase 3 is the effector caspase of the apoptotic pathway, which initiates the process of apoptosis upon receiving upstream activation signals. The PDB ID 4QTX was interacting through three hydrogen bonds and one pi-pi interaction with the 4-FPAC (Figure 5.3, Table 5.2.1). The amino acid Arg207 forms a hydrogen bond with the O and NH atom of benzene ring at a distance of 2.3 Å, NH group of His121 make a hydrogen bond with the 3-Oxo-butyraldehyde group of the ligand at a distance of 2.1 Å, Gly122 form hydrogen bond at a distance of 1.8 Å and one pi-pi interaction with Trp206. These interactions result in the docking score of -3.462 kcal/mol, Glide energy of -41.86 kcal/mol, Glide emodel of -61.51 kJ/mol and IFD score of -241.533 kcal/mol (Table 5.2). This direct interaction between 4-FPAC and caspase 3 induces the apoptotic death in the A549 cell line.

SNAIL

The result of Chapter 3 confirmed that 4-FPAC reduces metastasis through downregulation of the Snail transcription factor, which plays an important role in the downregulation of E-cadherin - an epithelial cell marker and upregulation of mesenchymal markers like vimentin and N-cadherin to promote EMT. *In vitro* study confirmed the involvement of PI3K/AKT/NF-κB

signaling in the downregulation of Snail mediated EMT in the A549 cell line. When 4-FPAC docked with the PDB ID, 4QLI, it generates a docking score of -2.89kcal/mol, Glide energy of -34.35kcal/mol, Glide emodel of -61.514kJ/mol and IFD score of -396.85kcal/mol (Table 5.2). It interacts with the ligand (4-FPAC) through two hydrogen bonds (Figure 5.3.1, Table 5.2.1) in which Lys122 -NH group interact with the oxygen atom of pentanoic acid methylamine moiety at a distance of 1.7 Å, followed by Arg129 -OH group which interact with the oxygen group of the 3-Methyl-but-3-enal group at a distance of 2.2 Å and special interactions such as pi-pi and pi-cation interactions with the Phe119 and Lys49 (benzene ring) (Table 5.2). The interaction between 4-FPAC and SNAIL might be blocking the binding of other TFs responsible for the transcription of E-cadherin to maintain the epithelial characteristics.

VEGFR

The *in vitro* study in the A549 cell line revealed (Refer Chapter 3) that there was no significant change observed in VEGF-α at the protein level, but the angiogenesis process was halted in the treatment group of 4-FPAC, therefore here in this chapter, the analysis of 4-FPAC on VEGF receptor was done using molecular docking. 4-FPAC efficiently docked into the active site VEGFR (5EW3) with a docking score of -9.66kcal/mol, Glide energy of -57kcal/mol, Glide emodel of -89.493kJ/mol and IFD score of -551.66kcal/mol (Table 5.2). The interaction with ligand includes two hydrogen bonds and one pi-cation interaction, Glu885 -hydrogen bond between the NH group of the ligand at the distance of 2.3 Å, Asp1046 form hydrogen-bond with the oxygen atom of the ligand at the distance of 2.8 Å. Lys868 form pi-cation interaction with the Fluoro-phenyl ring of the 4-FPAC (Figure 5.3.1, Table 5.2.1). The interaction of 4-FPAC is strong enough to block the binding of VEGF to VEGF-receptor and hamper the process of the neovascularization process, which is apparent in the results of the study explained previously (Chapter 3).

PTEN

PTEN act as a negative regulator of AKT, the downstream mediator of the PI3K signaling pathway. When PTEN gets activated, it hampers the activity of AKT and hence, the major pathway responsible for the proliferation and survival of cells. In cancer cells were the activity of AKT was increased either due to mutation or other factors, activation of PTEN can help to minimize its effect on the cellular processes. Hence, this is considered a good target for anticancer therapy. In Chapter 4, the effect of 4-FPAC on AKT and PI3K signaling pathway was evident, however, the effect of derivative on PTEN was predicted here, using molecular docking.

When 4-FPAC was docked with the PTEN (PDB ID; 5BZX) it generates docking score of -5.557 kcal/mol, Glide energy of -45.103kcal/mol, Glide emodel of -62.393kJ/mol and IFD score of -550.0842kcal/mol (Table 5.2). The interaction was made with three hydrogen bond (Figure 5.3.2, Table 5.2.1) that includes, Lys128 -NH group of amino acid interact with the oxygen atom of chromen ring at a distance of 2.6 Å, Gly129, Thr167 -H bond between NH group of amino acid and oxygen atom of the 3-Oxo-butyraldehyde group of the ligand at a distance of 2.1 Å (Figure 5.3.2, Table 5.2.1). It confirmed that along with upstream regulation, it' activity is also affected due to direct interaction with the 4-FPAC itself. This interaction might be activating the PTEN, which leads to a substantial decrease in the level of AKT, as observed in the Chapter 4.

HIF-1α

4-FPAC docked with the HIF-1α (PDB ID; 5L9B) with docking score of -8.893kcal/mol, Glide energy of -52.442kcal/mol, Glide emodel of -75.217kJ/mol and IFD score of -477.35kcal/mol (Table 5.2). Interaction between compound and ligand occurred with three hydrogen, and three pi-cation (Figure 5.3.2, Table 5.2.1), Thr303 -H bond between OH group of ligand and the oxygen atom of the formaldehyde group a distance of 2.5 Å and Thr387 -H bond between the same group of amino acid with the oxygen atom of the ligand at a distance of 2.67 Å, Tyr329 -H bond between NH of the amino acid and oxygen atom of the ligand at the distance of 2.8 Å. Benzene moiety formed pi-cation between the manganese metal and Arg383 NH group at a distance of 5.8 and 4.3 Å, and also interact with His313 and His374 followed by with Fluro-benzene moiety at a distance of 3.3 Å and also interact with MN501 through pi-cation interaction (Figure 5.3.2, Table 5.2.1). Such a large number of interactions might be responsible for the HIF-1α mediated regulation of metastasis in the A549 cell line.

DISCUSSION

Phytochemicals are always the richest source for the therapeutic intervention, but lower availability of active compounds and tedious process of extraction leads to the generation of chemical analog of the compound. Coumarin is one of them, which has many potential therapeutic properties, including anticancer. To increase its efficacy and to reduce its side effect, many analogs with different pharmacophores of coumarin were synthesized and screened for their anticancer property in many cell lines, including lung adenocarcinoma cell lines. In the present study, two series of coumarin derivatives (mono-substituted and di-substituted) with different pharmacophores at C-4 (mono-substituted) and C-3, C-7 (di-substituted) positions were synthesized and screened for their anticancer property in the A549 human lung cancer cell line

(Refer Chapter 1). Among all the derivatives, 4-Fluorophenylacetamide-acetyl coumarin was selected since it showed a lower median inhibitory concentration (0.16nM) in the A549 cell line. Moreover, when tested against non-cancerous mouse fibroblast cell line (NIH3T3), 0.16nM of 4-FPAC did not elicit any adverse effect (Durgapal et al., 2017). The *in vitro* study, as mentioned in Chapter 2, revealed that the 4-FPAC induces apoptosis through p53 dependent and caspase-mediated pathways that involve both the extrinsic as well as an intrinsic pathway of apoptosis. Therefore, p53, BAX, caspase 3, and caspase 8 were analyzed using *in silico* based molecular docking study. Similarly, the derivative 4-FPAC also reduces the metastasis and angiogenesis by p53 dependent Snail pathway (Refer Chapter 3). Further studies (Chapter 4) uncovered that the major signaling pathway behind the derivative's anticancer property is PI3K signaling pathway, hence, PTEN, a negative regulator of the PI3K pathway, was analyzed using molecular docking.

It was observed that 4-FPAC could effectively hamper cancer cell proliferation, metastasis, and angiogenesis at a very minimal dose without affecting the non-cancerous cell line. Therefore, further confirmation for its drugability and reactivity was investigated using, *in silico* based DFT calculations, ADME prediction, and Molecular Docking. Lipinski's Rule of Five was used to analyze the physicochemical properties of the compound and its druggability. It includes physiochemical properties, which are imperative as a basic necessity to pass the blood-brain barrier efficiently namely passive diffusion, includes molecular weight, lipophilicity, hydrogen bonding, and charge. When there is a violation of more than one Rule, it leads to poor ADME property. Drug molecules of molecular weight less than 500Da are easily transported, diffused, and absorbed as compared to larger molecules. The compound with high molecular weights is likely to have low solubility and have difficulty passing through the cell membrane (Srimai et al., 2013). Lipophilicity is an important parameter required by the drug candidate, which helps in crossing the hydrophobic phospholipid bilayer of the membrane. A balance of solubility and polar/hydrophobic properties is crucial for specific routes of absorption and crossing any biological barriers that a drug needs to penetrate to reach the desired site of action, in order to affect the specific event. For better oral bioavailability, lipophilicity (a ratio of the molecule's solubility in octanol to solubility in water) should be less than 5 (QlogPo/w≤5). When more than 5, H-bond donors, and more than 10 H-bond acceptors group exists, it further minimizes the bioavailability of the drug. In this study, we found that all the parameters are within the limit of Lipinski's Rule of Five (Table 5.3). The molecular weight of the compound is 355.3, comes within an acceptable range to have high solubility, and high probability of being able to enter a

cell. H bond donor group is only 1≤5, and the H bond acceptor group in 7.5≤10, as well as clogP (QPlogPo/w), is 2.3, which again ≤5. With all these parameters, 4-FPAC stands high in druggability rank.

Another important parameter for selecting a good drug candidate is its good pharmacokinetic property, i.e., ADME property. Nearly 40% of drug candidates fail in clinical trials due to poor ADME properties. These late-stage failures lead to rapid escalation in the cost of drug development. The early-stage elimination of flawed drug candidates can reduce the wastage of time and resources and streamline the overall process of drug development. Therefore, ADME predictions at the early stage of the development process can help in lowering the cost and appraising the performance of candidate drug molecules during clinical trials. The pharmacokinetic property includes Blood-Brain Barrier penetration or absorption and distribution. Caco-2 cell permeability represents drug metabolism, transport, and percentage of oral absorption. All the parameters were under the acceptable limit, with 1.27 (QPlogBB), 319.5 (QPPCaco), and 85.41% oral absorption property (Table 5.3). No violation of Lipinski's Rule of Five has been observed and all together with these results, 4-FPAC can be considered as a drug-like candidate with lesser toxicity and good bioavailability.

The electron density is considered a very important factor for understanding the reactivity of electrophilic and nucleophilic sites as well as the interactions of hydrogen bonding and molecular electrostatic potential of the compound (Scrocco and Tomasi, 1979). In DFT calculation, Molecular electrostatic potential theory is used for the prediction and forecasting of all the optimized sites of the molecule's reactive sites for electrophilic and nucleophilic attack. Therefore, for predicting this reactivity of nucleophilic and electrophilic sites for 4-FPAC, MESP was simulated using the B3LYP level of the optimized geometry. The different colors (red, blue, and light blue) at the MESP surface (Figure 5.2) represent different values of the electrostatic potential as the regions of most negative, most positive, and zero electrostatic potential, respectively. The negative electrostatic potential at the MESP (red) indicates that this region is attractive to the proton by the aggregate electron density in the molecule and corresponds to electrophilic reactivity (regions of most electronegative electrostatic potential). In contrast, the positive electrostatic potential (blue) is the region that is responsible for the repulsion of the proton by the atomic nuclei and corresponds to nucleophilic reactivity (regions of the most positive electrostatic potential). In contrast, the light blue shade represents regions of zero potential. In 4-FPAC the nucleophilic sites are lying on oxygen, and fluorine moieties, which are the electronegative compound and have a tendency to attract nucleophiles. On the other side,

electrophilic or positive potential sites are existing on hydrogen and methyl group of the compound, which again justifying the periodic property of hydrogen and methyl group in 4-FPAC. However, around the 4-FPAC nucleus, the electron density is equally distributed, making it electroneutral. Therefore, the MESP study helped in giving a clear vision about the electrostatic feature of the compound that might be the reason behind the biological effect of the 4-FPAC.

From the literature, it is known that the lower band-energy gap, which is the energy difference between two frontier orbitals ($\Delta E = E_{LUMO} - E_{HOMO}$), is critical for the chemical reactivity and kinetic stability of any molecule. In 4-FPAC, the highest occupied molecular orbital HOMO and LUMO energies were located on two distinct parts of the molecule. HOMO orbitals are located on the 4-Fluorobenzene ring, and LUMO orbitals are located on the 3-acetyl coumarin ring, indicating the active participation of the compound during protein-ligand interactions. The calculated HOMO-LUMO energy gap for 4-FPAC was -0.1378eV (Table 5.1), the low and negative Eigenvalues for band energy gap indicate that both rapid electrons transfer, as well as the exchange, is equally possible, this low energy gap making 4-FPAC chemically very reactive. Together, these results depicted the potential reactive site and also confirmed the highly reactive nature of the 4-FPAC.

HOMO represents the tendency to give electron, hence ionization potential is directly related to the HOMO energy. LUMO, on the other hand, represents the electron-accepting potential of the compound therefore, LUMO energy is directly related to the electron affinity (Gece, 2008; Fukui, 1982). By using ionization potential and electron affinity, quantum chemical descriptors, such as Softness, Chemical Hardness, Chemical Potential, Electronegativity, and Electrophilic Index, were calculated (Table 5.1.1). The higher value of ionization potential is predictive of higher stability and chemical inertness of the molecule, while the opposite characteristics are the representative of lower ionization potential. The chemical hardness indicates the resistance towards the deformation or polarization of the electron cloud of molecules. The hard molecule has a large energy gap, however, a soft molecule has a small energy gap (Pearson, 1988). Soft molecules are more reactive than the hard ones because they can release electrons quickly. 4-FPAC is showing lower ionization potential of -0.2430eV and higher value for chemical softness *viz.,* 7.26eV, indicating the lower stability and higher chemical reactivity of the compound. In contrast, the lower electrophilicity index ω=0.219eV (the tendency of chemical species to acquire electrons) and lower chemical potential μ=-0.174eV (an indicator of electrons escape; electrons escapes from high chemical potential to those have lower chemical potential) of 4-

FPAC signify it's potential to attract electron. Therefore the overall global reactivity descriptors reconfirming the Frontier Molecular Orbital (HOMO and LUMO) based prediction of 4-FPAC.

Since 4-FPAC is very reactive in nature, and *in vitro* study also revealed that 4-FPAC was affecting the apoptosis, metastasis, and angiogenesis via key regulators like p53, BAX, caspase 3, caspase 8, Snail, HIF-1α and VEGFR, the major pathway behind its anticancer effect was predicted to be PI3K signaling pathway. Therefore, *in silico* based molecular docking was done to reaffirm the above findings. From the results of *in silico* study, we found that the 4-FPAC is highly reactive in nature, and when docked with p53, it gives docking score of -5.89 kcal/mol and interacting with amino acids, *viz*., Lys132, Arg273, Arg248, Arg280 and Ala276, with six hydrogen bonds and with Arg273 via two pi-pi bonds (Figure 5.3, Table 5.2.1). BAX, a pro-apoptotic protein of the BCL-2 family is critical for the outer mitochondrial permeabilization, release of cytochrome c, and initiation of apoptosis, which is directly activated by p53 and permeabilize the mitochondria (Chipuk et al., 2004). The *in vitro* study revealed that there is a loss of mitochondrial membrane potential and upregulation in BAX and the *in silico* study also confirmed that 4-FPAC interact with BAX (Figure 5.3, Table 5.2), and generated docking score -11.7kcal/mol by two H-bond with amino acid Trp17 and Gly166 and three pi-pi interactions with Phe165 which could be responsible for BAX induced release of cytochrome c from mitochondria (Table 5.2.1). Activated BAX also upregulated the caspase 8, which cleaves the caspase 3 into cleaved caspase 3 and activates the intrinsic pathway of apoptosis. The *in silico* molecular docking strategy confirmed the interaction of 4-FPAC with caspase 8 and 3. The caspase 8 interact with two stable H-bond (Figure 5.3, Table 5.2.1) with the active site amino acid residue Asn138 and Ser109 and generates a docking score of -5.563kcal/mol. However, it interacts with caspase 3 with three hydrogens and two pi-pi interactions (Figure 5.3, Table 5.2.1), and generates docking score of -3.462kcal/mol which is less negative than the caspase 8, which signify that 4-FPAC induces caspase 8 more strongly than the caspase 3 and it is caspase 8 whose activity is responsible for the activation of caspase 3 functions.

4-FPAC interact with SNAIL to perform its anti-metastasis function via two hydrogen bonds (Lys122 and Arg129) and special interactions such as pi-pi and pi-cation interactions with the Phe119 and Lys49 (benzene ring). With this interaction, it generated a docking score of -2.89kcal/mol (Figure 5.3.1, Table 5.2, Table 5.2.1). The interaction is not very strong as compare to other PDBs, which explains why the E-cadherin and vimentin did not show any significant alteration upon 4-FPAC treatment. Similarly, VEGFR is also docked with compound and

showed a docking score of -9.66kcal/mol and interacted with two hydrogen and one pi-cation at the active site of the amino acid *viz.*, Glu885, Asp1046, and Lys868 (Figure 5.3.1, Table 5.2.1). The docking score and interaction might have placed the ligand at the active pocket or near the site at which VEGF binds due to which it is not able to bind with the VEGFR to initiate the angiogenesis in 4-FPAC treated cells. HIF-1α a mediator of hypoxia-induced activation of VEGF to initiate the neovascularization process. It was activated in the 4-FPAC treated cell line, however, this increase was not apparent in the VEGF expression. At docking with 4-FPAC, the PDB generates docking score of -8.893kcal/mol with three hydrogen bonds and three pi-cation interaction (Figure 5.3.1, Table 5.2, Table 5.2.1) which might present at the active site through which angiogenic mediator interacts.

PTEN a negative regulator of the PI3K signaling pathway (PI3K/AKT pathway). When gets activated, it downregulates the intrinsic pathway of apoptosis by phosphorylating pro-apoptotic gene BAX and BAD activates MDM2, thereby downregulate the p53 and hampers all the pathway regulated by p53 including that of metastasis. *In silico* study revealed that 4-FPAC interact with active site amino acid Lys128, Gly129, and Thr167 by three H-bond (Figure 5.3.2, Table 5.2, Table 5.2.1) and gives docking score of -5.557kcal/mol which supplement the *in vitro* finding that 4-FPAC not only affecting the AKT but also PTEN and its cumulative effect leads the anticancer activity of 4-FPAC.

The overall finding demonstrates that *in silico* molecular docking study is a powerful technique to study the action of many key molecules involves in potentiate the anticancer effect of any compound. Herein, we have done an *in silico* molecular docking study to supplement the *in vitro* findings in which the interaction of compound 4-FPAC with key molecules *viz.*, p53, BAX, caspase 8, caspase 3, SNAIL, VEGFR, PTEN, and HIF-1α were analyzed. The result revealed that the 4-FPAC is directly interacting with these molecules and ensuing its desired effect. The corresponding sites of reactivity and highly reactive nature of the compound were uncovered in MESP and HOMO-LUMO studies. Drug-likeliness and ADME property of 4-FPAC revealed that compound has good drug-likeliness and ADME property with high oral absorption quality. Therefore, it can be taken further as a novel chemotherapeutic agent for future anticancer drug development.

SUMMARY

4-FPAC, a synthetic derivative of coumarin, which has a substitution of Fluorophenylacetamide at the C-4 position of acetylated basic coumarin ring. The *in vitro* based data suggested the anti-proliferative, anti-metastasis, and anti-angiogenic properties of the 4-FPAC at a very minimal dose of 0.16nM with lesser side effects on the non-cancer cells of mouse origin, NIH3T3. This chapter summarizes the *in silico* part of the study which was used to analyze, the druggability and safety of 4-FPAC, if consumed orally using ADME and knowledge-based set of rules, the Lipinski's Rule of Five. The chemical reactivity, biological activity, and kinetic stability of 4-FPAC was prophesied using DFT calculations and interactions with the targeted PDBs was established using the molecular docking protocol of Schrödinger. The ADME property of 4-FPAC was analyzed using QikProp module of Schrödinger software suite. The 4-FPAC showed good ADME as well as satisfied all the criteria of drug likeliness based on Lipinski's Rule of Five. The frontier molecular orbitals, HOMO, and LUMO, were analyzed for their corresponding energies as well as their energy gaps using Jaguar version 9.8 (Schrödinger). 4-FPAC showed a negative value of E_{HOMO} -0.2430eV and E_{LUMO} -0.1052eV as well as the lower energy gap (ΔE) of -0.1378eV which signify its high chemical reactivity as well as the biological activity. MESP map also created to check its electron density distribution around the different molecules in the compound. On the basis of, FMO, several global reactivity descriptors were also generated to check its chemical behavior and found that 4-FPAC has tendency to gain as well lose an electron to perform its reactions. Based on the *in vitro* finding of previous chapters, the key mediators were docked using molecular docking protocol Glide (version 6.7) with the 4-FPAC to check its molecular interactions. Molecular docking revealed that 4-FPAC directly interacting with PDB IDs; 5LGY (p53), 2K7W (BAX), 4ZBW (caspase 8), 4QTX (caspase 3), 5EW3 (VEGFR), 4QLI (SNAIL), 5BZX (PTEN) and 5L9B (HIF-1α) to exerts its effects. Overall, the *in silico* based study confirmed that the 4-FPAC has good druggability, ADME properties. It also supports the highly reactive nature of the compound, as deduced from the *in vitro* based findings, and can be taken further for as a novel chemotherapeutic for the development of a future anticancer drug. The entire work and results are graphically summarized in Figure 5.4.

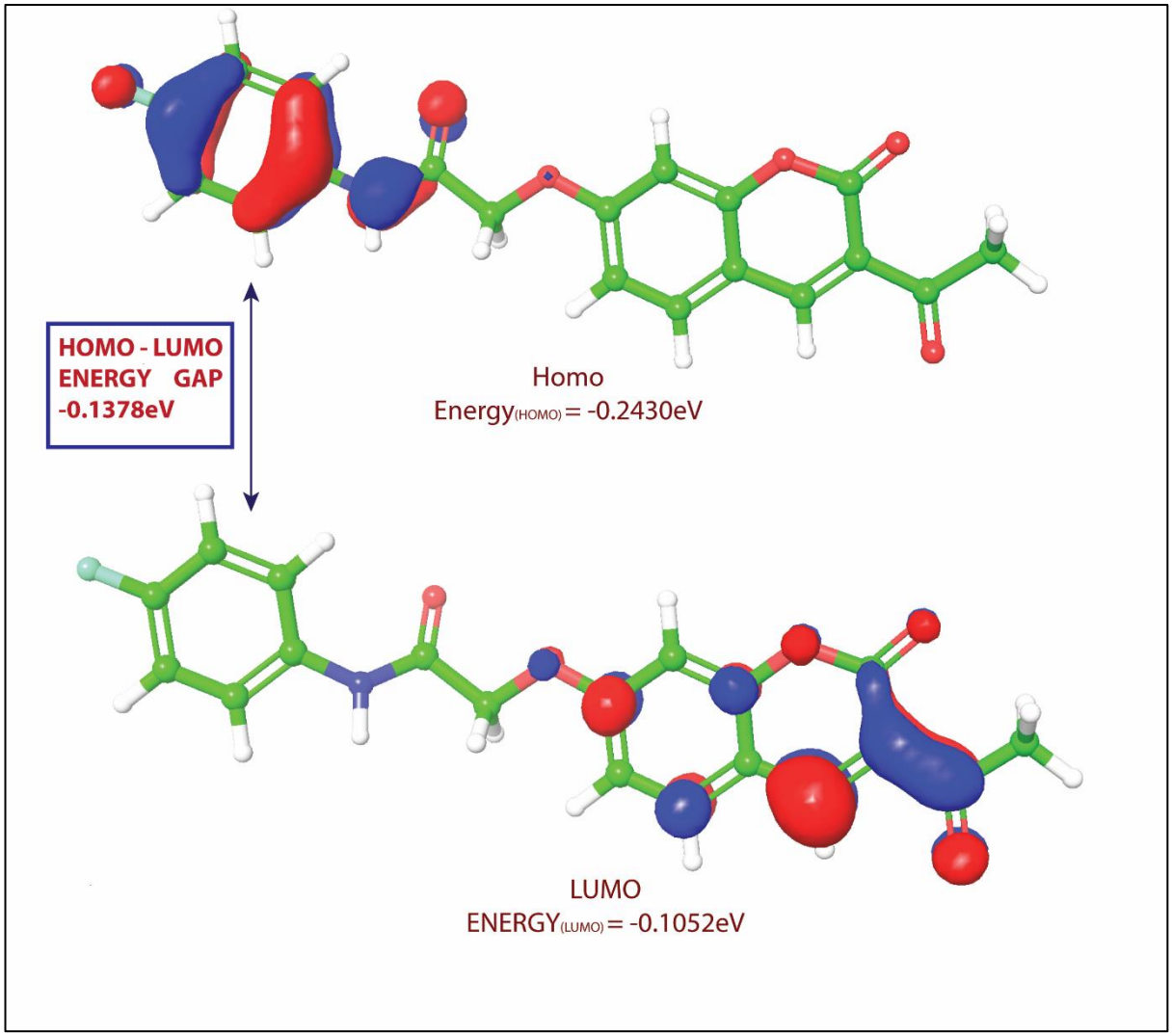

Figure 5.1. Frontier Molecular Orbital (HOMO-LUMO) distribution of 4-FPAC and their corresponding energies; HOMO orbital is distributed on the 4-Fluorobenzene ring, and LUMO orbital on the 3-acetyl coumarin ring of the 4-FPAC and their corresponding energies are E_{HOMO} = -0.2430eV, E_{LUMO} = -0.1052eV and ΔE= -0.1378eV respectively.

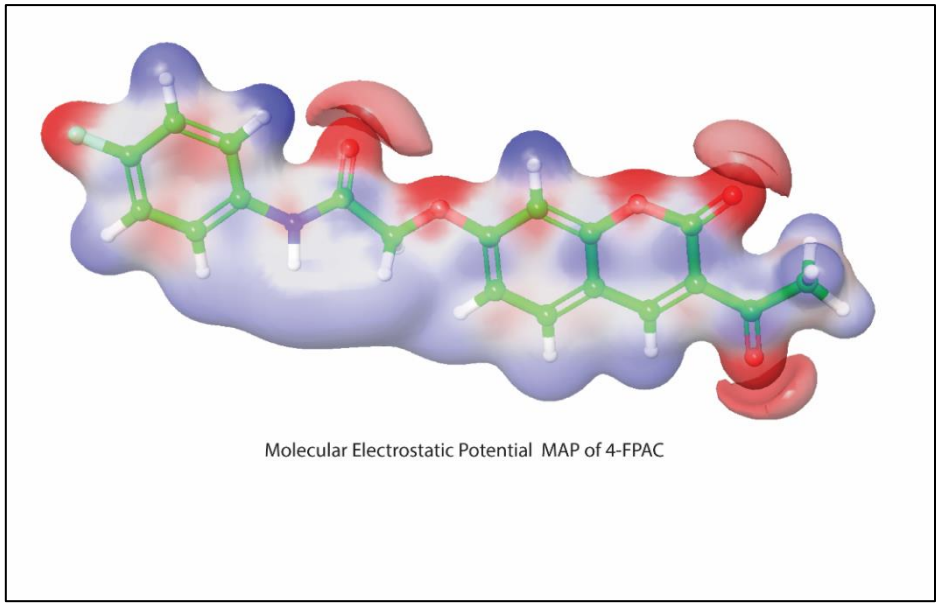

Figure 5.2. MESP Map of the 4-FPAC; the calculated electrostatic potential surface on the compound color code -192.2281 a.u (deepest red) and -23.1788 a.u. (deepest blue). The most positive electrostatic potential region is deep blue, and the most negative electrostatic potential region is dep Red in color. B3LYP functional and 631G**++ level basic set.

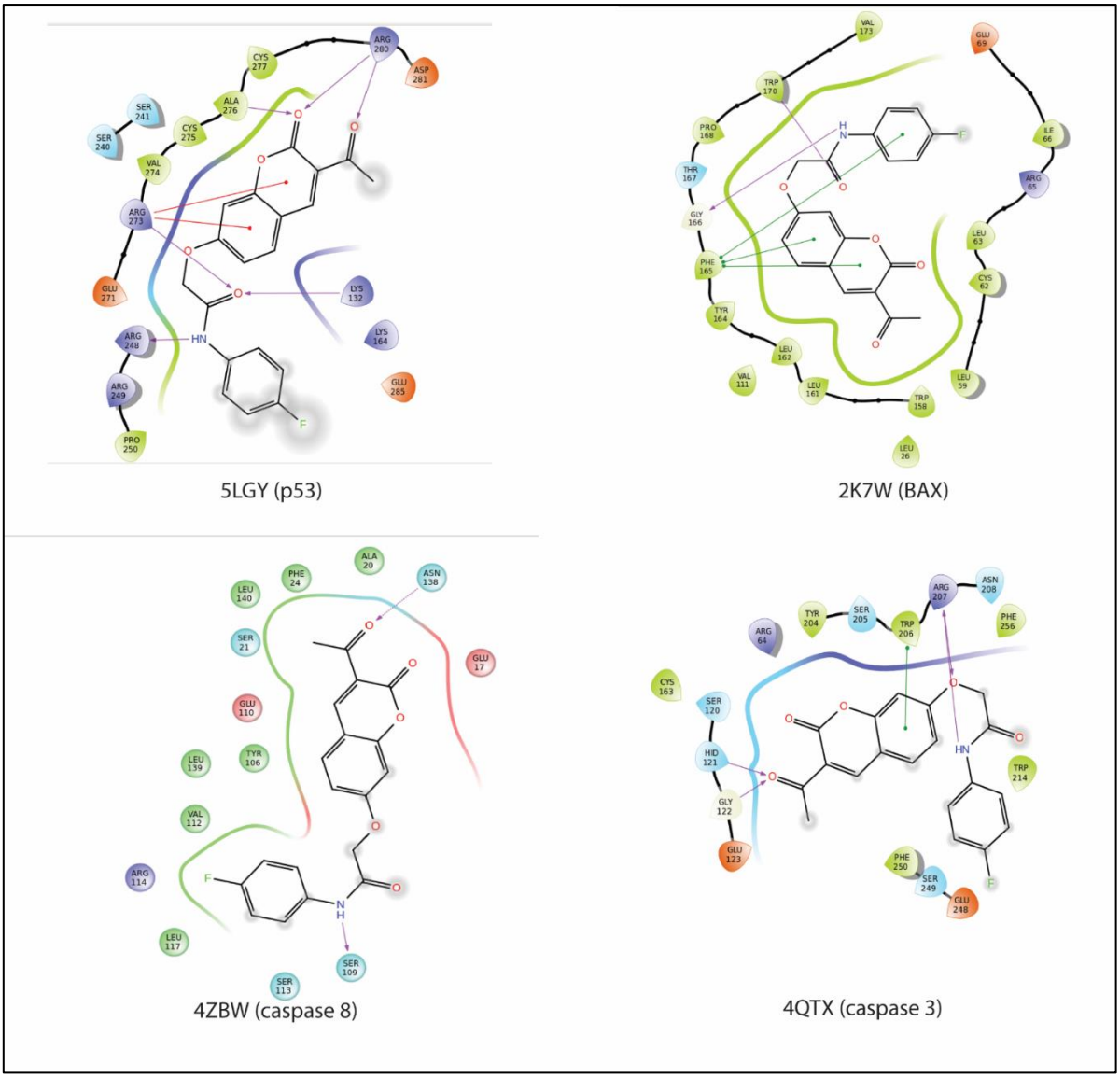

Figure 5.3. 2D interaction diagram of 4-FPAC with p53 (5LGY), BAX (2K7W), caspase 8 (4ZBW) and caspase 3 (4QTX) displaying hydrogen bond with the side chain (magenta dotted line), hydrogen bond (magenta line) π-π stacking (green line) and π-cation (red line) interactions.

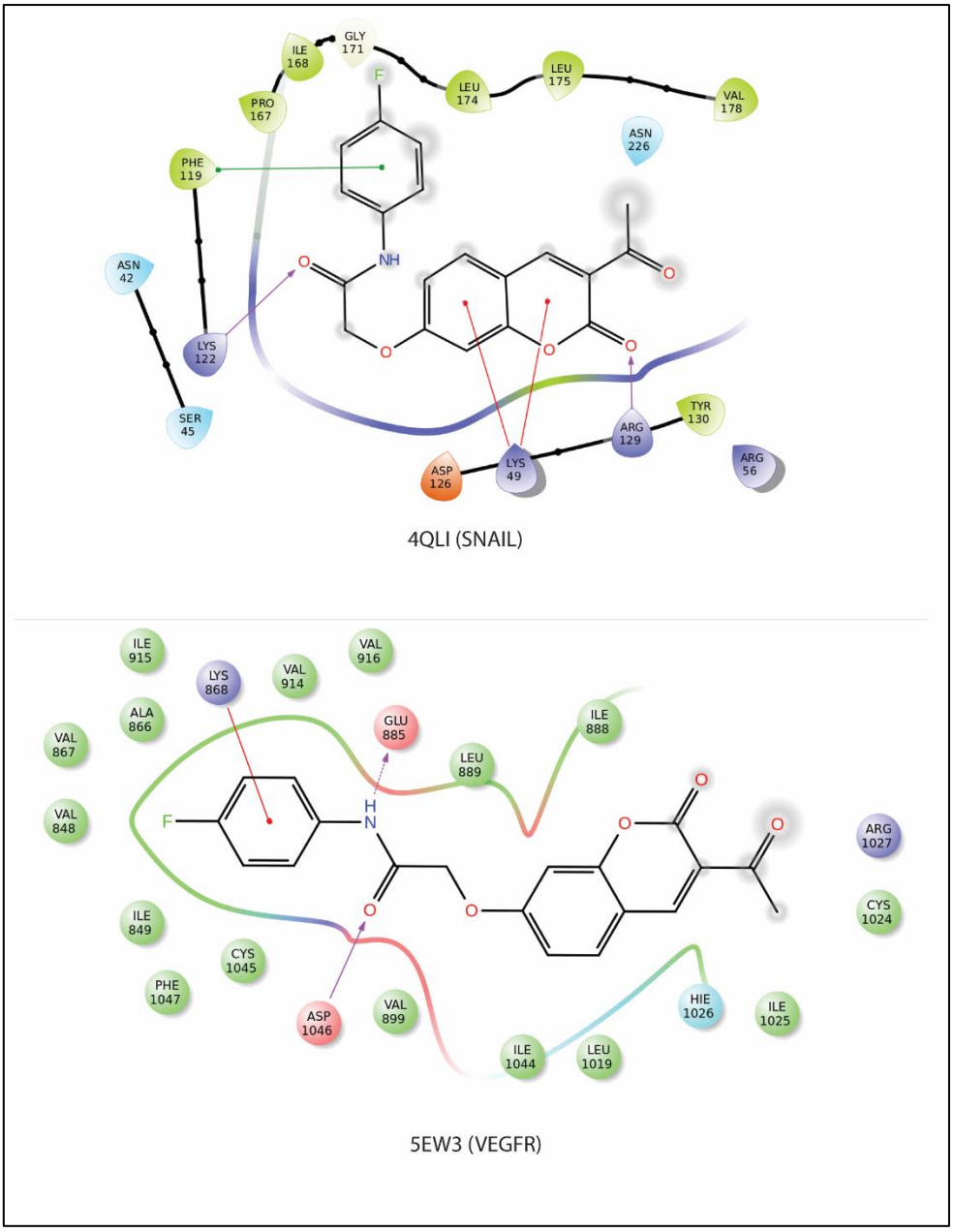

Figure 5.3.1. 2D interaction diagram of 4-FPAC with SNAIL (4QLI) and VEGFR(5EW3) displaying hydrogen bond with the side chain (magenta dotted line), hydrogen bond (magenta line) π-π stacking (green line) and π-cation(red line) interactions.

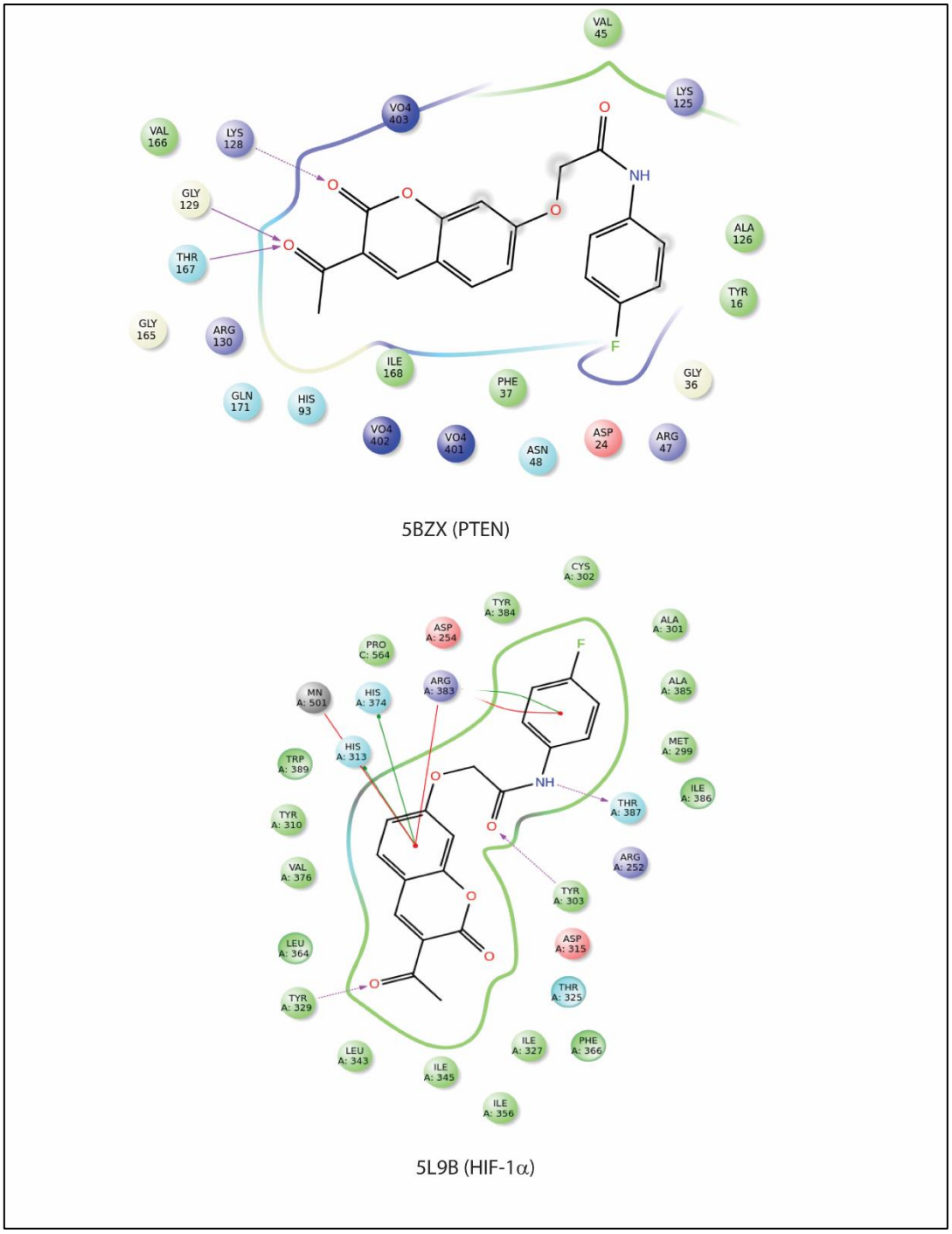

Figure 5.3.2. 2D interaction diagram of 4-FPAC with PTEN (4BZX) and HIF-1α (5L9B) displaying hydrogen bond with the side chain (magenta dotted line), hydrogen bond (magenta line) π-π stacking (green line) and π-cation (red line) interactions.

DFT calculations (Frontier Molecular Orbital density field)	
Energy$_{HOMO}$	-0.2430eV
Energy$_{LUMO}$	-0.1052eV
HOMO-LUMO Energy Gap (ΔE)	-0.1378eV
Salvation Energy	-1263.2kcal/mol

Table 5.1. Frontier Molecular Orbital (HOMO and LUMO) and related transition energy (HOMO-LUMO energy gap) of 4-FPAC calculated using Jaguar version 9.8 (Schrödinger).

Reactive descriptors	Equations	4-FPAC
Ionization Potential (I)	$-E_{HOMO}$	0.2430eV
Electron Affinity (A)	$-E_{LUMO}$	0.1052eV
Chemical Hardness (η)	$\eta = (I - A)/2$	0.0689eV
Chemical Softness (S)	$S = 1/2\eta$	7.26eV
Chemical Potential (μ)	$\mu = -(I + A)/2$	-0.174eV
Electronegativity (χ)	$\chi = (I + A)/2$	0.174eV
Electrophilic Index (ω)	$\omega = \mu^2/2\eta$	0.219eV

Table 5.1.1. Frontier Molecular Orbital based quantum chemical descriptors of 4-fluorophenylacetamide-acetyl coumarin derivative. The parameters were calculated from the equations based on the Koopman's theorem for closed-shell molecules.

Protein (PDB ID)	Docking score (kcal/mol)	IFD score (kcal/mol)	Glide energy (kcal/mol)	Glide emodel (kJ/mol)
p53 (5LGY)	-5.89	-420	-48.0	-67.9
BAX (2K7W)	-11.7	-436.558	-50.78	-65.94
caspase 8 (4ZBW)	-5.56	-441.533	-42.05	-54.187
caspase 3 (4QTX)	-3.462	-241.533	-41.86	-61.51
SNAIL (4QLI)	-2.89	-396.85	-34.359	-61.514
VEGFR (5EW3)	-9.66	-551.66	-57.0	-89.493
PTEN (5BZX)	-5.557	-550.08	-45.103	-62.393
HIF-1α (5L9B)	-8.893	-477.35	-52.442	-75.217

Table 5.2. Molecular docking study of 4-FPAC with PDB IDs; p53, BAX, caspase 8, caspase 3, SNAIL, VEGFR, PTEN and HIF-1α using Glide, 6.7, Schrödinger, LLC, New York, NY, 2015. Table representing the Docking score (kcal/mol), IFD score (kcal/mol), Glide Energy (kcal/mol) and Glide emodel (kJ/mol).

Protein (PDB ID)	Bond Interaction	Amino acid interacting with 4-FPAC
p53 (5LGY)	6 H-Bond and 2 pi-pi interaction	Lys 132, Arg273, Arg248, Arg280, Ala276, Arg273
BAX (2K7W)	2 H-Bond and 3 pi-pi interaction	Trp17, Gly166, Phe165.
caspase 8 (4ZBW)	2 H-Bond	Asn138, Ser109
caspase 3 (4QTX)	3 H-Bond and 1 pi-pi interaction	Arg207, His121, Gly122, Trp206
SNAIL (4QLI)	2-H bond and one salt bridge	Lys122, Arg129, Phe119, Lys49
VEGFR (5EW3)	2 H-Bond and 1 pi-pi interaction	Glu885, Asp1046, Lys868.
PTEN (5BZX)	3 H-Bond	Lys128, Gly129, Thr167.
HIF-1α (5L9B)	3 H-Bond and 3 pi-pi interaction	Thr303, Thr387, Try329, Arg383, His313, His374

Table 5.2.1. Molecular docking study of 4-FPAC; table representing the bond interactions between amino acids present at the active site of PDBs and ligand (4-FPAC).

Descriptors	**Range of 4-FPAC**	**Acceptable range** (range is for 95% of known drugs)
Molecular weight	355.3	130-725
No of H-bond Donors	1	0-6
No of H-bond acceptors	10	2-20
QPloPo/w	2.329	-2-6.5
QPlogPoct	18.76	8-35
QPlogPw	12.56	4-45
QPlogS	-4.51	-6.5- 0.5
QPlogBB	-1.271	-3-1.2
QPlogHERG	-6.35	above -5
QPPMDCK	260.94	<25 is low; >500 is great
QPPCaco	319.6	<25 is low; >500 is great
Human Oral Absorption	3	1-low, 2-medium, 3-high
Percentage Human Oral Absorption	85.41%	>80% is high; <25% is low
Violation of Rule of Five	0	Maximum 4
Overall CNS activity	-2	-2 (inactive) to +2 (active)

Descriptors	**Range of 4-FPAC**	**Acceptable range** (range is for 95% of known drugs)
QPlogKhsa	-0.168	-1.5- 1.5
QPlogKp	-2.79	-0.8 - -1.0
#rtvFG	1	0-2
SASA	641.783	300-1000
FOSA	113.884	0-750
FISA	157.254	7-330
PISA	323.62	0-450
PSA	109.88	7-200

Table 5.3. Pharmacokinetics prediction of 4-FPAC using QuikProp 4.4; Table representing the ADME properties of the cell, and drug likeliness prediction using Lipinski's Rule of Five. QPlogPo/w, QPlogPoct, QPlogPw, QPlogS, QPlogBB; predicted partition coefficient of octanol/water, octanal/gas, water/ gas, aqueous solubility, and brain/blood, respectively. QPPMDCK and QPPCaco; predicted apparent cell permeability in MDCK and Caco-2 cell nm/sec. QPlogHERG; The predicted IC_{50} value for the blockage of HERG K^+ channel. Human Oral Absorption; qualitative human oral absorption based on a knowledge-based set of rules, Percentage Human Oral Absorption; quantitative prediction based on multiple linear regression model. QPlogKhsa, QPlogKp; predicted human serum albumin binding and skin permeability. #rtvFG; no of the reactive functional group. SASA, FOSA, FISA, PSA; Total solvent accessible surface area, a hydrophobic component of the SASA, hydrophilic component of the SASA, Polar nitrogen, and oxygen van der Waals surface area.

GRAPHICAL SUMMARY

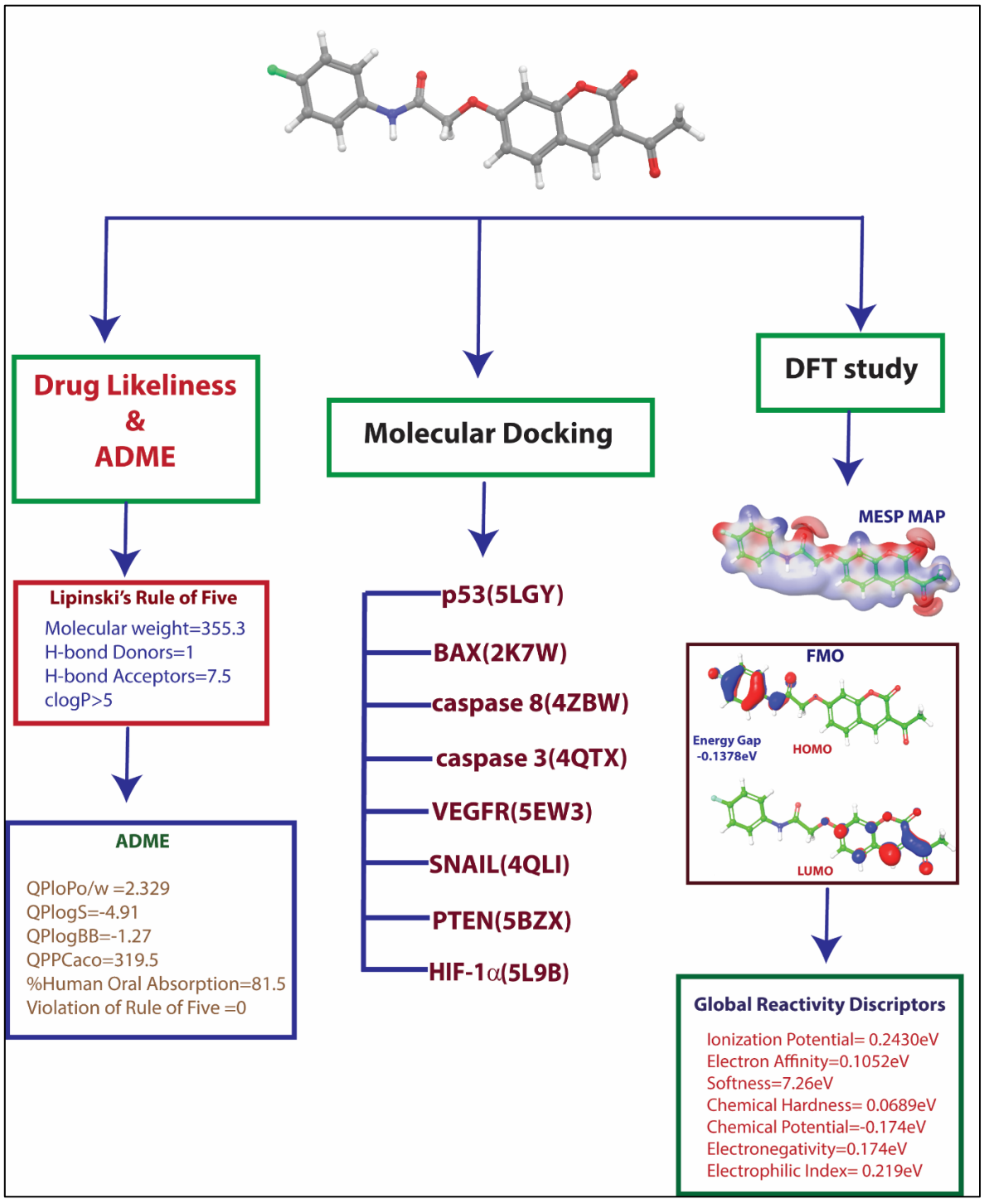

Figure 5.4. *in silico* study of 4-FPAC